ANALYSIS OF GEOMETRIC AND ORTHOGONAL CORRECTION ACCURACY FOR CAS-500 SATELLITE IMAGES

Y. Lee [1], T. Kim [1, 2] *

[1]Program in Smart City Engineering, Inha University, Incheon, S. Korea - eyoojin2@inha.edu, tezid@inha.ac.kr
[2] Dept. of Geoinformatic Engineering, Inha University, Incheon, S. Korea – tezid@inha.ac.kr

Commission I, WG I /4

KEY WORDS: CAS-500, KOMPSAT-3A, Precise Image, Precise Orthoimage, Sensor Model, Position Accuracy.

ABSTRACT:

This paper reports on geolocation accuracy of image products generated from Precision Image Processing (PIP) system developed for CAS-500 Satellite images. CAS-500, launched on 22 March, 2021, will be used mainly for land monitoring and 1:5000 scale mapping over the Korean Peninsula. For this purpose, ground control points (GCPs) and a Digital Terrain Model (DTM) have been collected over the Peninsula and integrated into the PIP for the generation of precision image product in an automated manner. The goal of this paper is to analyze the geolocation accuracy of image products generated from the PIP. Target geolocation accuracy of the PIP was set as 2 pixel RMSE using the internal GCP DB and DTM. Since CAS-500 images were not distributed yet, the analysis was performed using 13 KOMPSAT-3A satellite images, having similar specifications to CAS-500. The result showed that the accuracy of precise sensor models were about 1.797 pixels in South Korea and 1.907 pixels in North Korea. The accuracy of orthoimages were about 1.24 meters in South Korea and 1.59 meters in North Korea. Overall, the geolocation over North Korea was not as good as that over South Korea. It was judged that the quality of GCPs and DTM over North Korea affected the geolocation accuracy and, however, the accuracy gap was not too severe. The PIP system should produce image products within the targeted geolocation accuracy when CAS-500 delivers high resolution images over the Korean Peninsula.

1. INTRODUCTION

CAS-500, which launched in March 2021, is a 500kg medium-sized satellite (Han et al., 2017; Han et al., 2018). It carries a high-resolution camera to acquire images at 50cm Ground Sampling Distance (GSD) in panchromatic band and 2.2m GSD in multispectral bands. It is well-known that geolocation accuracy of satellite images is important for utilization of satellite images (Jeong., 2015). In particular, as satellites that can acquire high-resolution data have diversified, geolocation accuracy analysis and its improvement methods have been studied according to satellite image types. Location accuracy of EOC images acquired from KOMPSAT-1 was reported to be within 1 pixel (approximately 4 to 6 meters in space) when improved by precisely measured GCPs. The geometric accuracy analysis of KOMPSAT-3 images (Jeong et al., 2014) and KOMPSAT-3A images (Nyamjargal et al., 2017) were analyzed. Other authors reported accuracy analysis and improvement for satellite images, including QuickBird (Noguchi et al., 2004), SPOT-5 (Büyüksalihe et al., 2005), IKONOS (Dial et al., 2003), GeoEye-1 and WorldView-2 images (Aguilar et al., 2014).

It is important to analyze the geolocation accuracy of image products generated from CAS-500 images. For CAS-500, the Precision Image Processing (PIP) system has been developed for establishing precise sensor models and generating orthoimages (Kim, 2020). In particular, the PIP is equipped with GCP and DTM database over the Korean Peninsula enabling automated and systematic generation of high-quality image products (Park et al., 2020). In this paper, we report on the geolocation accuracy of image products from the PIP processed through the internal GCP and DTM DB. It is notable that matters concerning the composition and development of the PIP system have been reported in another paper (Park et al., 2020).

Since CAS-500 was in an Early Operation stage at the time of writing and its images were not distributed yet, the geolocation accuracy analysis was carried out using KOMPSAT-3A images. KOMPSAT-3A images have similar specifications as CAS-500 images. It was expected that this study can predict accuracy of precise image products produced from CAS-500.

Initial sensor models were established first from Rational Polynomial Coefficients (RPCs) provided with the KOMPSAT-3A images. Next, GCPs for the incoming images were automatically generated by matching the KOMPSAT-3A images against images chips within GCP DB. They were used to update initial RPCs and establish precise sensor models. Next, orthoimages were generated using DTM DB incorporated within the PIP. A total of 13 KOMPSAT-3A images were used for accuracy analysis.

2. METHOD

2.1 Data

The GCP DB within the PIP consists of 23,142 points over South Korea, 25,205 points over North Korea, and 1,539 points over the border. For each GCP point, an image chip centered at the point was prepared. The quality of GCP chips determines the quality of matching between the GCP chip and incoming satellite images. The quality of ground coordinates of GCPs determine the accuracy of precise sensor model. GCP DB used in experiments has specifications as Table 1.

* Corresponding author

Property	South Korea	North Korea	Border
Ground Coord.	UCP, TP	IP	IP
Raw Data	Aerial orthoimage	Satellite orthoimage	Satellite orthoimage
Geographic Coord.	WGS84	WGS84	WGS84
Projection Coord.	UTM-K	UTM-K	UTM-K
Chip Band	RGB	Grey	Grey
Chip GSD	0.25m	1.0m	0.5m
Chip Size (pixel)	1027 X 1027	257 X 257	513 X 513

Table 1. Properties of used GCP Chip (UCP: Unified Control Point, TP: Triangulation Point, IP: Image Point).

KOMPSAT-3A satellite images used for experiments have specifications as Table 2.

Property	Specification	
Satellite	KOMPSAT-3A	
Product Level	Level 1R	
Ground Sample Distance	PAN	0.55 m (nadir)
	MS	2.2 m (nadir)
Swath Width	12 km (nadir)	
Image Size	(about) 24060 X 19000 pixel	
Bit Per Pixel	16bit	

Table 2. Properties of KOMPSAT-3A.

2.2 Geolocation Accuracy Analysis Method

The process of geolocation accuracy analysis by sensor model and output is shown in Figure 1.

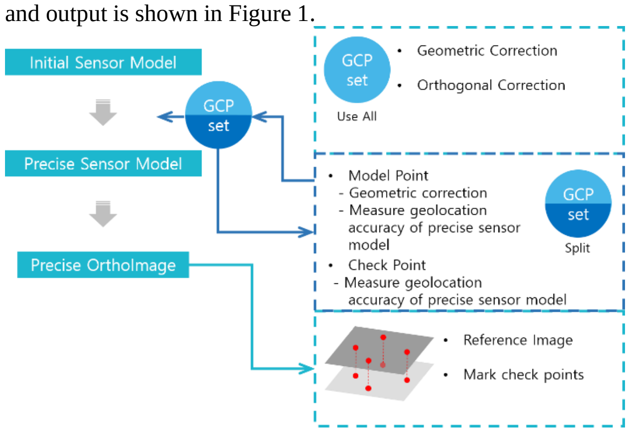

Figure 1. Process of geolocation accuracy analysis.

First, we established initial sensor models with initial RPCs provided with images and defined relationship between image coordinates and ground coordinates of images. Next, reference points were automatically acquired through GCP chip matching (Shin et al., 2018). They were visually checked and, if necessary, manually adjusted. Resulting GCPs were split to model points and check points. Model points were used for establishment of a precise sensor model and check points for accuracy analysis. To update the initial RPC, we used a first-order polynomial model in form of affine models as shown in the following formula (Jeong and Kim, 2014).

$$\Delta p = a_0 + a_c \cdot Column + a_r \cdot Row \qquad (1)$$

$$\Delta r = b_0 + b_c \cdot Column + b_r \cdot Row \qquad (2)$$

where Δp and Δr represent adjusted values in column and row directions, respectively, and a_0, a_c, a_r, b_0, b_c, b_r adjustment parameters estimated by least squares regulation. Figure 2 and Table 3 show comparison before and after precise sensor modelling. As shown in the figure 3-(b), the ground coordinates of matched image point was moved as close as possible to the ground coordinates of the gcp chip.

Finally, we generated orthoimages using the precise sensor models and DTM DB. We obtained separate check points manually from orthoimage database and used them for accuracy analysis of orthoimages.

Figure 2. View of GCP chip(center of the red cross: ground coordinates of GCP).

	
(a) Before calibrating the matched image's gcp	(b) After calibrating the matched image's gcp

Table 3. Comparison of calibrating GCPs.

3. RESULT AND DISCUSSIONS

3.1 Accuracy of Precise Sensor Models

Figure 5 and 6 shows the location of GCPs generated from the PIP. As mentioned above, we divided GCPs into model and check GCPs. We focused on dividing the points as uniform batches for accurate accuracy measurements. In the figures, model points were represented by circles and check points by triangles.

Table 4 and 5 show the accuracy of precise sensor models using model points. Table 6 and 7 show the accuracy of precise sensor models using check points. Since different dataset were used over

Sound and North Korea for GCP DB establishment, the accuracy was analysed over South and North Korea, accordingly.

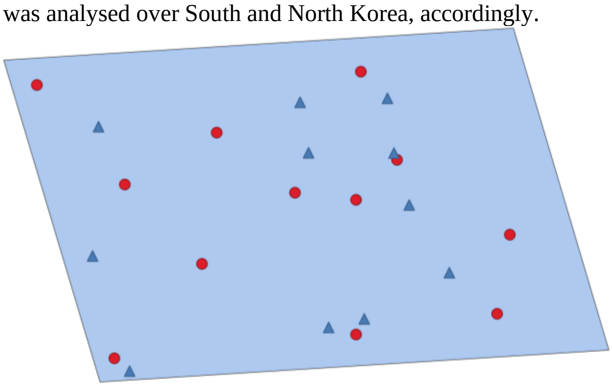

Figure 3. GCP distribution of South Korea, Seoul.

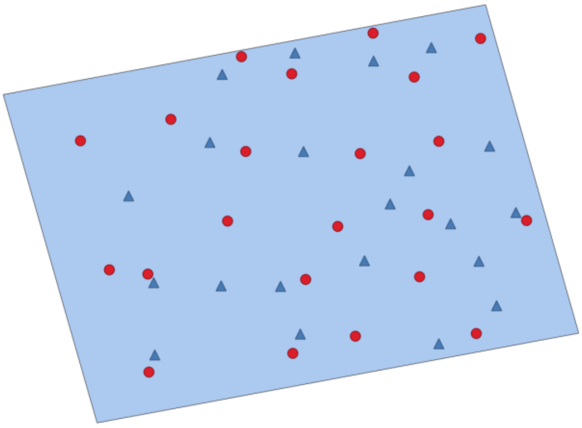

Figure 4. GCP distribution of North Korea, Pyeongyang.

South Korea	Max initial Error (pixel)	RMSE (pixel)
Seoul	3.69	1.809
Gyeonggido	2.46	1.38
Incheon	2.31	1.463
Gyeongsangbukdo	3.98	1.733
Chungcheongnamdo	1.5	1.007
Jejudo	1.65	1.002
Average		**1.399**

Table 4. Model point geolocation accuracy of precise sensor model (South Korea).

North Korea	Max initial Error (pixel)	RMSE (pixel)
Wonsan	3.88	2.099
Shinuiju	1.95	0.985
Pyeongyang	4.18	2.655
Hamheung	4.05	1.834
Gaeseong	3.27	1.953
Gangwondo	2.27	1.615
East Sea	2.67	1.361
Average		**1.786**

Table 5. Model point geolocation accuracy of precise sensor model (North Korea).

South Korea	Max initial Error (pixel)	RMSE (pixel)
Seoul	3.79	2.108
Gyeonggido	4.46	1.838
Incheon	5.57	2.587
Gyeongsangbukdo	2.68	1.502
Chungcheongnamdo	2.77	1.345
Jejudo	3.09	1.401
Average		**1.797**

Table 6. Check point geolocation accuracy of precise sensor model (South Korea).

North Korea	Max initial Error (pixel)	RMSE (pixel)
Wonsan	2.8	1.579
Shinuiju	2.57	1.302
Pyeongyang	4.77	2.627
Hamheung	3.91	1.978
Gaeseong	3.35	1.866
Gangwondo	3	1.923
East Sea	4.49	2.606
Average		**1.983**

Table 7. Check point geolocation accuracy of precise sensor model (North Korea).

As shown in Table 6 and 7, accuracy of precise sensor model measured 1.797 pixel over South Korea, and 1.983 pixel over North Korea. Accuracy measurements of North Korea have shown that comparably low than that of South Korea due to quality of GCPs. It is well known that GCP distribution and placement affect accuracy of sensor model (Kim et al., 2000). The East Sea image includes mountainous areas with uneven GCP distribution, which resulted in low accuracy. Figure 7 and 8 show check point errors graphically. The blue dots represent the true location of GCPs, and the red dots the estimated location of GCPs by the sensor model.

This contribution has been peer-reviewed.
https://doi.org/10.5194/isprs-archives-XLIII-B1-2021-57-2021

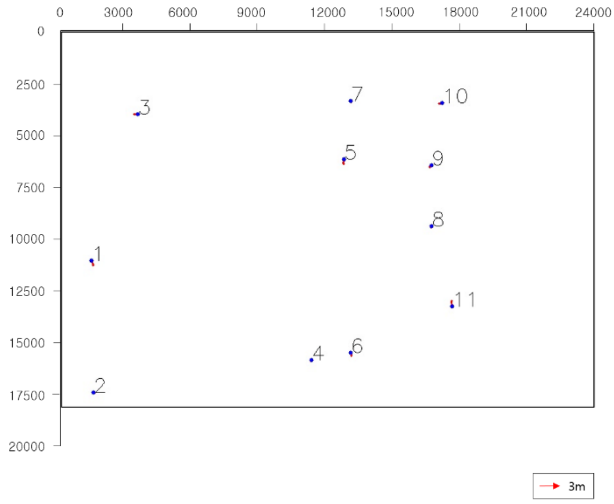

Figure 5. Geometric errors of check point - Seoul

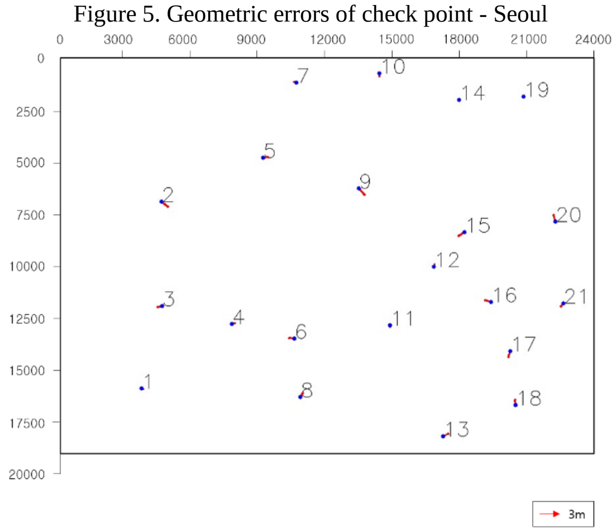

Figure 6. Geometric errors of check point – Pyeongyang.

In case of Seoul (Figure 7), most of the red dots and blue dots overlapped, confirming that the sensor model was established with great precision. In case of Pyeongyang, there were slight separations between the red dot and the blue dot. As a result, we could judge the quality of GCP was low than that of South Korea, leading slightly inferior quality of sensor model.

3.2 Accuracy of Orthoimages

After generating precise sensor models, we performed ortho-rectification. We used a DTM at spatial resolution of 5m by NGII (National Geographic Information Institute). And then, we selected feature points within aerial orthoimage database as verification points as to analyze geolocation accuracy of precise orthoimages. To measure geolocation accuracy, we extracted identical image points to verification points. We extracted one check point for each divided segment, except the segment that were difficult to identify check points such as mountain area. And then, we measured horizontal position error. Table 8 and 9 show geolocation accuracy of orthoimages. Figure 9 and 10 show geometric errors in precise orthoimage of Seoul and Pyeongyang images.

South Korea	Col Err	Row Err	RMSE (m)
Seoul	1.06	0.59	1.21
Gyeonggido	0.49	1.12	1.23
Incheon	0.57	0.68	0.89
Gyeongsangbukdo	1.71	0.74	1.87
Chungcheongnamdo	0.57	0.71	0.91
Jejudo	0.87	0.99	1.32
Average			**1.24**

Table 8. Geolocation accuracy of precise orthoimage (South Korea).

North Korea	Col Err	Row Err	RMSE (m)
Wonsan	2.16	0.63	2.25
Shinuiju	1.65	0.96	1.91
Pyeongyang	1.42	2.62	2.98
Hamheung	0.79	0.86	1.17
Gaeseong	0.56	0.75	0.94
Gangwondo	1.22	1.32	1.8
East Sea	1.39	0.41	1.45
Average			**1.786**

Table 9. Geolocation accuracy of precise orthoimage (North Korea).

As shown Table 8 and 9, accuracy of orthoimages over South Korea was 1.24 pixel, and that of North Korea was 1.6 pixel. Both sites showed accuracy numbers within our target value. The precise orthoimage of East Sea was located in North Korean border region and most of the image contained mountain areas. Errors may have occurred in process of extracting check points. This may have contributed to the large error of the ortho-rectified East Sea images.

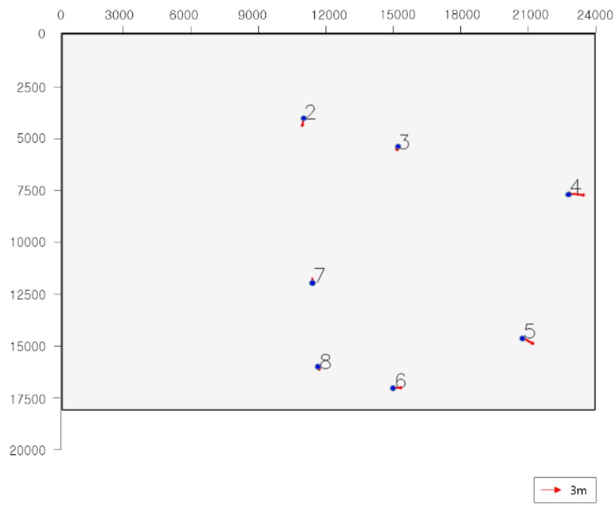

Figure 7. Geometric errors in precise orthoimage of Seoul compared with aerial orthoimage.

https://doi.org/10.5194/isprs-archives-XLIII-B1-2021-57-2021 | © Author(s) 2021. CC BY 4.0 License.

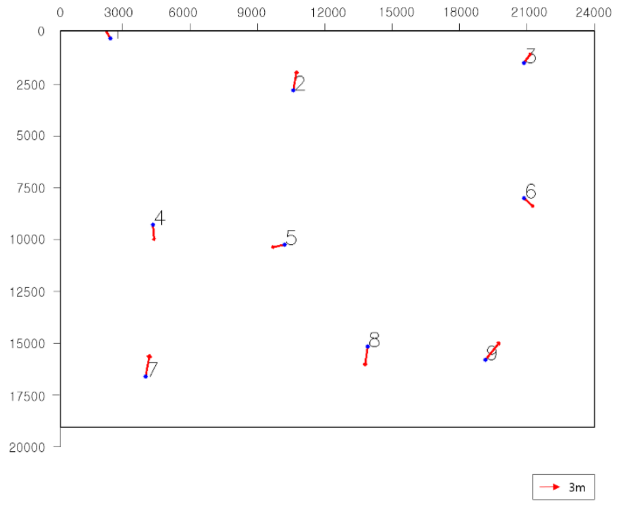

Figure 8. Geometric errors in precise orthoimage of Pyeongyang compared with aerial orthoimage.

Figure 9 and 10 show the geolocation errors of the Seoul and Pyeongyang orthoimages. It is possible to check relatively lower accuracy of Pyeongyang image. Figure 11 shows enlarged overlap between the Chungcheongnamdo orthoimage and digital map. It show correctness of boundaries between orthoimage and digital map.

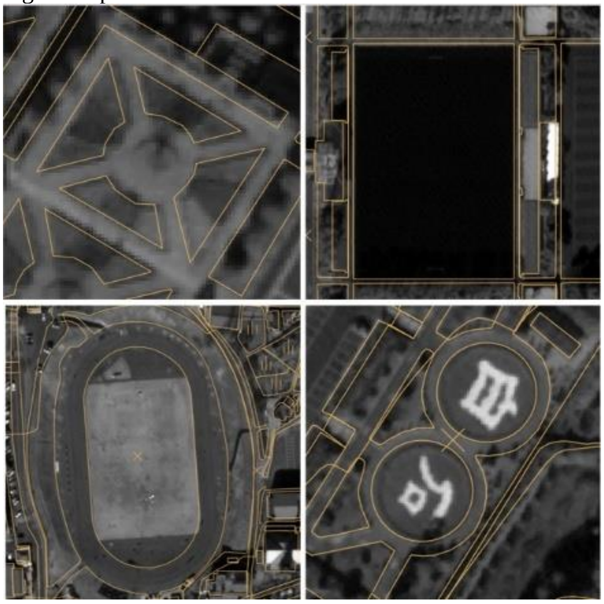

Figure 9. Enlarged Chungcheongnamdo orthoimage with overlaid digital map.

4. CONCLUSIONS

This paper analysed the accuracy of geometric correction and orthogonal correction of the Precision Image Processing system developed for CAS-500. Using KOMPSAT-3A images, we tested images over South and North Korea and showed precise sensor model accuracy with an average under 2 pixels, which was our research goal. In case of precise orthoimage accuracy, it showed an average accuracy of less than 2m. However, in case of North Korea, due to low quality of GCPs, precise sensor model accuracy and orthoimage accuracy tended to be lower than the case of South Korea. Nevertheless, the analysis results indicated that the PIP system developed could produce high quality images products from CAS-500 images.

REFERENCES

Dial, G., H. Bowen, F. Gerlach, J. Grodecki, and R. Oleszczuk, 2003. Ikonos satellite, imagery, and products, Remote Sensing of Environment, 88(1- 2): 23-36.

Aguilar, M.Á., M. Saldaña, and F.J. Aguilar, 2014. Generation and quality assessment of Stereo-Extracted DSM from Geo-Eye-1 and WorldView-2 imagery, IEEE Transaction of Geoscience and Remote Sensing, 52(2): 1259-1271.

Jeong, J. and T. Kim, 2014. Analysis of dual-sensor stereo geometry and its positioning accuracy, Photogrammetric Engineering and Remote Sensing, 80(7): 653-662.

Nyamjargal. E., J. Kim and T. Kim, 2017. Analysis of Geometric and Spatial Image Quality of KOMPSAT-3A Imagery in Comparison with KOMPSAT-3 Imagery, Korean Journal of Remote Sensing, 33(1): 1~13.

Han, C.Y., Kim, J., and Kim, S.S., 2017. Optimised Design of Standard Platform for CAS500 satellite, *The Society for Aerospace System Engineering*, 219-220.

Büyüksalih, G., G. Koçak, H. Topan, M. Oruç, and A. Marangoz, 2005. Spot revisited: accuracy assessment, DEM generation and validation from stereo Spot-5 HRG images, The Photogrammetric Record, 20(110): 130-146.

Han, C.Y., Kim, J., and Kim, S.S., 2018. Trade-off Study of Mechanical Design for CAS500 satellite, *The Society for Aerospace System Engineering*, 252-253.

Noguchi, M., C.S. Fraser, T. Nakamura, T. Shimono, and S. Oki, 2004. Accuracy assessment of Quick Bird stereo imagery, The Photogrammetric Record, 19(106): 128-137.

Jeong, J., 2015. Comparison of single-sensor stereo model and dual-sensor stereo model with high resolution satellite imagery, *Korean Journal of Remote Sensing*, 31(5): 421-432 (in Korean with English abstract).

Shin, J.I., Yoon, W.S., Park, H.J., Oh, K.Y., and T. Kim, 2018. A Method to Improve Matching Success Rate between KOMPSAT-3A Imagery and Aerial Ortho-Images, Korean Journal of Remote Sensing, 34(6-1): 893-903 (in Korean with English abstract).

Kim. T, 2020. Current Research and Development Status for CAS 500-1/2 Image Processing and Utilization Technology, *Korean Journal of Remote Sensing*, 36(5-2): 861-866.

Park, H., J.H. Son, H.S. Jung, K.E. Kweon, K.D. Lee and T. Kim, 2020. Development of the Precision Image Processing System for CAS-500, Korean Journal of Remote Sensing, 36(5-2): 881-891 (in Korean with English abstract).